ChemComm

COMMENT

View Article Online
View Journal | View Issue

Cite this: *Chem. Commun.*, 2023, 59, 5293

Comment on "Fluorimetric sensing of ATP in water by an imidazolium hydrazone based sensor" by S. Farshbaf and P. Anzenbacher Jr., *Chem. Commun.*, 2019, 55, 1770†

Sakshi Sareen, Agnieszka Wiśniewska, Karina Kwapiszewska * and Robert Hołyst *

Received 12th January 2023,
Accepted 31st March 2023

DOI: 10.1039/d3cc00175j

rsc.li/chemcomm

In the paper, "Fluorimetric sensing of ATP in water by an imidazolium hydrazone based sensor," Farshbaf and Anzenbacher presented the application of bisantrene as a fluorescent ATP sensor in organic–inorganic mixtures of solvents. Encouraged by the results presented in the parent study, we aimed to apply this strategy for physiologically relevant water-based buffers and – preferably – intracellular application. Here we present the results of our investigations and point to the limitations of bisantrene applications *in vivo* as the ATP sensor.

Introduction

Quantifying ATP levels in living cells is an intensively sought-after tool in biochemistry and molecular biology. Fluorometric ATP sensors allow, in principle, quantification of ATP concentration in cells.[1] A potent chemical biosensor for ATP quantification in living systems is still lacking. The reference study[2] for this commentary underlines bisantrene salt as a potential ATP sensor based on their interaction in TRIS:DMSO buffer. Our research aimed to evaluate the usability of bisantrene as a chemical sensor for ATP in physiologically relevant media and inside living cells. We found that cellular uptake of bisantrene is hindered due to the occurrence of large aggregates in the medium surrounding the cells. We confirmed bisantrene crystal formation in different media using polarisation and fluorescence microscopy. We also show how bisantrene crystallization affects UV-VIS spectrophotometry in TRIS:DMSO and PBS.

Anthracene analogs like bisantrene have been known to possess the ability to hinder cell proliferation, ROS generation, and caspase-3 activation, which are significant markers for initiating apoptosis.[3] Bisantrene has been used as an anti-cancer drug to treat acute myeloid leukemia,[4] breast cancers,[5] and many others since the late 1980s. Recent pharmaceutical development has led to the reintroduction of this drug in synergy with others as a novel drug for tumor treatment. With an established cytotoxicity profile of the drug already known, we decided to study bisantrene as an ATP sensor in cell-based experiments. 2 μM bisantrene was added to human embryonic kidney (HEK293) and human cervix carcinoma (HeLa) cells, preferably to investigate drug-ATP interaction in an intracellular environment. Studies suggest that anthracene and its derivatives fluoresce between $\lambda_{ex/em}$: 300/500 nm.[6,7] We checked the fluorescence of bisantrene-treated cells under the confocal microscope. We used 405 nm and 488 nm excitation lasers, and only the 488 nm excitation provided a fluorescence signal from the bisantrene (Fig. 1A). Referring to fluorescence maxima observed in the parent study, we observed 2 μM bisantrene in the DAPI channel (λ_{ex} = 405 nm) to detect fluorescence, if any. We observed no fluorescence at 405 nm wavelength in PBS solution. A small population of fluorescent HEK cells with 1 μM bisantrene in PBS was detected using a confocal microscope after excitation from a blue laser (λ_{ex} = 488 nm) (ESI,† Fig S4C). Similar experiments were performed on HEK293 and HeLa cells

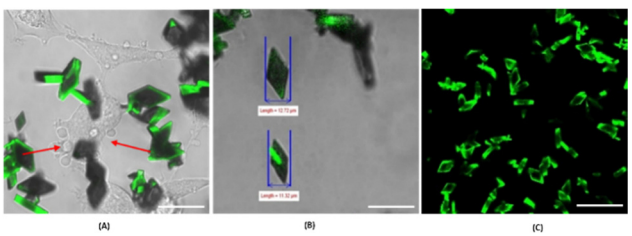

Fig. 1 Confocal images of bisantrene salt. (A) Fluorescence of bisantrene salt imaged upon excitation at 488 nm on HEK cells with apoptotic bodies (red arrows) formed after 20 min of drug addition. (B) Bisantrene crystal dimensions in μm (~12 μm). (C) 2 μM fluorescent bisantrene crystals in PBS with λ_{ex} = 485 nm. Scale bar: 100 μm.

Institute of Physical Chemistry, Polish Academy of Science, Kasprzaka Street, Warsaw 01-224, Poland. E-mail: rholyst@ichf.edu.pl

† Electronic supplementary information (ESI) available. See DOI: https://doi.org/10.1039/d3cc00175j

to verify whether the results could be correlated in different cell lines. The fluorescent cell population was significantly low compared to the number of non-fluorescent cells. Moreover, fluorescent species were mainly present outside the cells, forming large aggregates of regular shapes. This led us to hypothesize that bisantrene forms crystals in the physiologically-relevant media.

In the late 1980s, it was discovered that bisantrene's intravascular injections resulted in precipitation at the deposition site in the body. This specific drug behavior was explained as the co-crystallization of bisantrene chloride with water molecules in the presence of pyridium chloride.[8] We suspect similar crystallization behavior *in vitro* in the presence of buffers containing soluble ions like magnesium and calcium chloride. We confirmed the presence of bisantrene crystals using polarization microscopy. At 25 °C, needle-shaped and tetrahedron-like crystals were detected in water and PBS, respectively. Needle-shaped crystals disappeared after increasing the temperature from 25 °C to 36 °C in water. This could be due to the increased solubility of bisantrene crystals in water at a higher temperature. Needle-shaped crystals disappeared completely at 36 °C (the temperature required for cell growth in culture conditions). Only tetrahedron-shaped crystals remained by the end of the first temperature cycle, which ended at 80 °C. Needle-shaped crystals reappeared when the temperature was gradually brought down from 80 °C to 36 °C at intervals of 3 °C every 5 min. The recrystallization resulted in the reduction of crystal size. Similar experiments were performed with bisantrene crystals in PBS and TRIS:DMSO (Fig. 2B and D). Bisantrene crystals remained tetrahedron in shape (without any needle-shaped crystal formation) in PBS and TRIS:DMSO buffers. The two types of crystal morphologies observed can be due to interactions between molecules and ions (water, calcium chloride, and magnesium chloride, respectively), which need not be regularly planar in all conformations. This could result from having a crystallographic inversion center about bisantrenium ions in buffers.[8]

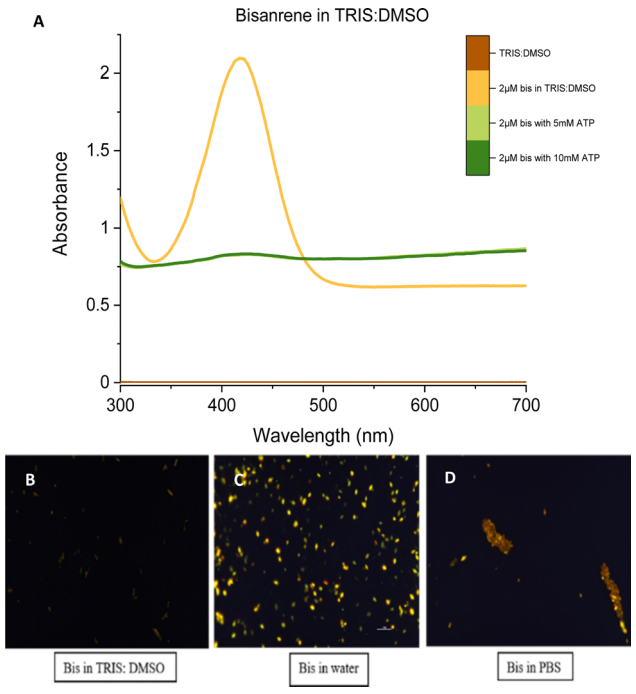

Fig. 2 Bisantrene salt analysis in different buffers. (A) Absorbance maxima for bisantrene salt in TRIS:DMSO was obtained at 410 nm. (B–D) 2 μM of bisantrene was analysed in different water-based buffers at 36 °C. The images shown in the panel were recorded at t_0, 36 °C.

Bisantrene samples containing different concentrations of ATP were checked in water and PBS buffers. No changes were reported in the crystals' shape, size, solubility, or fluorescence. Results for 2 μM bisantrene with 1 mM ATP in TRIS:DMSO, water, and PBS are shown in ESI,† Fig S5.

We also examined absorbance spectra (300–700 nm) for bisantrene in different buffers. For TRIS:DMSO buffer, we obtained a spectrum corresponding to the one observed in the parent study (Fig. 2). The same measurement was performed in a water-based PBS buffer—however, when the DMSO-based stock solution was dissolved in PBS, increased opacity following quick precipitation and sedimentation of crystals was observed. The solution contained a lot of suspended particles, making it more opaque and thus impairing absorbance measurements. We infer that the presence of crystals was responsible for light scattering. Therefore, the absorbance measurements refer to the sum of the sample's absorption and scattering (extinction). This resulted in decreased apparent absorbance of the solution when the salt started settling down (see ESI,† Fig. S8). Absorbance/Extinction measurements for 2 μM bisantrene in TRIS:DMSO is shown in Fig. 2.

We also performed time-correlated single photon counting (TCSPC) studies in PBS buffer (TCSPC data, refer to ESI,† Fig S6). The singular and intense peak was observed in TCSPC time traces for bisantrene in PBS samples, indicating the presence of large and bright aggregates/crystals (refer to ESI,† Fig S4(b)).

Considering the action of bisantrene as an anti-tumor agent, we wanted to visualize the drug's uptake by comparing the drug's size and target. The size of bisantrene crystals in PBS and the area of HeLa cells were measured. Fig. 1B shows the length of bisantrene crystals (~12 μm) as measured in comparison to HeLa cells (Refer to ESI,† Fig S7B and C). We found that the bisantrene crystal-to-cell size ratio is ~1, which may explain our observation of cells' minimal uptake of bisantrene. Cellular uptake of bisantrene was almost negligible in HEK as well as HeLa cells. Bisantrene concentrations as low as 2 μM proved toxic to HEK 293 cells within 20–30 minutes after addition (refer to ESI,† Fig S9). Cells began detaching from the glass slide during this time. Cells attached to the surface after 30 min had some bisantrene crystals/aggregates attached to the cell membrane. On close observation, apoptotic bodies could be seen in HEK293 cells after 20 min of bisantrene addition (Fig. 1A). We also observed a green fluorescent signal from the extracellular environment. It was unclear if the signal was due to bisantrene-induced cell lysis or from the free molecules of bisantrene interacting with each other in the extracellular environment. In the case of cell lysis, we assume the released ATP from cells could have interacted with the free bisantrene molecules to exhibit a fluorescence signal. To negate the effect of cell lysis, 2 μM bisantrene (in PBS) was excited using λ_{ex} = 488 nm to correlate fluorescence signals observed in the case of free bisantrene-bisantrene molecule interaction.

A green fluorescent signal was recorded from a compact shape corresponding to bisantrene crystals/aggregates observed in polarisation microscopy (refer to Fig. 2D).

Conclusions

Confocal and polarization studies indicate that bisantrene forms crystals in water-based buffer solutions, which are the source of fluorescence in the visible spectrum. ATP binding with these crystals does not change their fluorescence. The size of these salt crystals in PBS buffer solution was of the same magnitude as that of the cell, which made the uptake of these crystals by mammalian cells impossible. From our experiments, we conclude that the application of bisantrene as an ATP sensor in living cell models is unlikely in a physiologically relevant water-based buffer.

Author contributions

SS, KK, and RH designed the study; SS performed experiments; SS and AW performed and concluded polarisation microscopy measurements. SS and KK analysed the data, and SS, KK, and RH drafted the manuscript.

Conflicts of interest

There are no conflicts to declare.

Acknowledgements

This work was supported by the National Science Centre, Poland, within the grant OPUS UMO-2019/33/B/ST4/00557.

Notes and references

1 M. Tantama, J. R. Martínez-François, R. Mongeon and G. Yellen, Imaging energy status in live cells with a fluorescent biosensor of the intracellular ATP-to-ADP ratio, *Nat. Commun.*, 2013, **4**, 2550.
2 S. Farshbaf and P. Anzenbacher, Fluorimetric sensing of ATP in water by an imidazolium hydrazone based sensor, *Chem. Commun.*, 2019, **55**, 1770–1773.
3 C. G. Pierpont and S. A. Lang, Crystallographic characterization of the anticancer drug bisantrene cocrystallized with pyridinium chloride, *Acta Crystallogr., Sect. C: Cryst. Struct. Commun.*, 1986, **42**, 1085–1087.
4 B. C. Valdez, *et al.*, Synergism of the Anthracene-Derivative Anti-Cancer Agent Bisantrene with Nucleoside Analogs and A Bcl-2 Inhibitor in Acute Myeloid Leukemia Cells, *J. Clin. Exp. Oncol.*, 2021, **10**, 4.
5 S. N. Olsen and S. A. Armstrong, It's Not What You Say But How You Say It: Targeting RNA Methylation in AML, *Mol. Cell*, 2020, **78**, 996–998.
6 H.-Y. Yap, *et al.*, Bisantrene, an Active New Drug in the Treatment of Metastatic Breast Cancer, *Cancer Res.*, 1983, **43**, 1402–1404, **http://aacrjournals.org/cancerres/article-pdf/43/3/1402/2415887/cr0430031402.pdf**.
7 E. Liu, X. Liu, Z. Jin and F. Jian, Study on the relationship between structure and fluorescence properties of anthracene derivatives, *J. Mol. Struct.*, 2022, **1252**.
8 M. Uejima, *et al.*, A designed fluorescent anthracene derivative: Theory, calculation, synthesis, and characterization, *Chem. Phys. Lett.*, 2014, **602**, 80–83.